

Path Planning for Robotic Hypertrophic Laser Scar Therapy

Lilly Chiavetta

Department of Electrical Engineering

Pratt School of Engineering, Duke University

Durham, NC

lhc24@duke.edu

Kaelyn Pieter

Department of Mechanical Engineering and Material Science

Pratt School of Engineering, Duke University

Durham, NC

kmp101@duke.edu

Abstract—This paper discusses the application of robot learning methods to a surgical procedure utilizing lasers to encourage the body’s natural healing response, thus helping patients recover from hypertrophic scarring. It evaluates multiple segmentation techniques in combination with a greedy algorithm and tabular Q-Learning to enable autonomous scar identification and treatment planning. Experimental results demonstrate that the proposed model can accurately identify scar regions and generate effective path plans for a hypothetical surgical procedure.

I. INTRODUCTION

Laser-based skin repair procedures are an excellent method for the treatment of hypertrophic scars resulting from burn injuries, offering measurable improvements in scar pliability, pigmentation, and patient comfort [1], [5]. These scars, characterized by excessive collagen and raised tissue can vary greatly in shape and texture across different patients. As a result, every laser therapy session is unique and must be adapted to the patient’s anatomical presentation. Laser therapy for burn injuries involves creating controlled micro-wounds to stimulate tissue remodeling, a process that can be painful [1]. The central problem addressed in this project is how to design an autonomous robotic system capable of performing a laser surgery on hypertrophic scars. Our goal is to create an algorithm that can reliably perceive scars and create an appropriate path within the scar with safety and precision.

Although laser therapy is an essential scar treatment, its delivery requires extensive training, specialized equipment, careful intraoperative judgment, and prolonged procedures [1], [5]. A robotic system capable of generalizing optimized treatment paths, minimizing total laser exposure while maximizing therapeutic efficiency, could reduce clinical burden and expand access to care. Advances in artificial intelligence have demonstrated that scar appearance and severity can be assessed and predicted from clinical images [2], suggesting similar opportunities for algorithmic optimization in treatment planning and execution. By allowing for safe and effective laser operation, a robotic system could widely benefit the population of burn patients who otherwise would face limited or delayed treatment access.

Despite limited work directly targeting robotic laser remodeling of hypertrophic scars, related research in robotic tattooing and tattoo removal provides a promising foundation

for this problem. Modern tattoo robots, such as Blackdot, uses multiple dots of tattoo ink, rather than strokes, to create its designs and tackle the challenge of working with skin due to its plasticity [3]. Tattoo removal systems employ color thresholding to segment the tattoo apart from skin [4]. To path plan, they use a point-defined method to minimize thermal damage to the patient [4]. These studies and products illustrate the feasibility of robust perception and point-based path planning for laser interaction with human skin.

However, adapting these concepts to hypertrophic scar laser surgery remains challenging. Scar tissue is highly heterogeneous, with variations in thickness, vascularity, and optical properties that complicate sensing [2]. Laser procedures also generate heat; an improper path plan can cause a thermal injury, therefore it is key that the automated path planning must be temperature aware with a precise heat model [1], [5].

These factors create a complex and safety-critical environment for automation. This project aims to address these challenges by creating an autonomous system that integrates precise wound segmentation and temperature-aware path planning to simulate laser scar therapy. By adapting strategies from tattoo robotics and combining them with advances in image processing, this project aims to advance dermatology with robot learning and lay the groundwork for future clinical work in scar therapy.

II. METHODOLOGY AND IMPLEMENTATION

This project was implemented with 4 main parts: image segmentation, post-segmentation processing, a hypertrophic scar heat model, and surgery path planning. The code implementing these methods can be found in Appendix A.

A. Segmentation

To find the most ideal way to segment out hypertrophic scars from skin, 4 segmentation methods were tested: unsupervised gaussian mixture model (GMM) segmentation, using a pretrained ResNet-18 to extract spatial features, utilizing the pretrained SegmentAnything Model (SAM) [6], and finetuning a U-Net with a pretrained ResNet-34 encoder backbone.

1) *Unsupervised Segmentation*: Given that tattoo removal robots use color thresholding to segment out the tattoo to be removed from the skin [4], it was hypothesized that a GMM

method based on clustering pixels of a similar color would give a good level of accuracy. The GMM was implemented by fitting the model to a feature space that combined both color and spatial coordinates for each pixel. Spatial coordinates were scaled down and appended to pixel colors to form a 5-dimensional feature vector for each pixel. A GMM of three clusters (assuming one for skin, one for scar, and one for background) was then fitted to these features, and each pixel was assigned a label corresponding to its most likely cluster. This approach allowed for the model to capture both color similarity and spatial proximity. This combination works well for blobs of color in the image with harsh boundaries, so it may not be accurate on all scars because of their wide color variance.

2) *Pretrained ResNet-18*: Another method of segmentation meant to extract spatial features of the scar image is a pretrained ResNet-18 model with its last two layers removed in order to get a spatial feature map output. The pretrained weights chosen were from ImageNet since the dataset is quite robust [7]. A main limitation of this dataset is that it does not include scars so it is hypothesized that this will likely not have the accuracy necessary for clinical use.

3) *SegmentAnything Model*: In order to take advantage of a pretrained model already built for segmentation, the SAM built by Facebook [6] was tested for accurately segmenting scar tissue from skin. Two pretrained checkpoints were used: ViT-B (91 million parameters) and ViT-H (636 million parameters) [6]. Because scar location can differ in each image, automatic segmentation masks were generated, removing the need for prompting across test images.

4) *Fine Tuned U-Net*: A fourth method for segmentation of the scars is fine-tuning a U-Net with a pretrained ResNet-34 encoder. This approach leveraged transfer learning by initializing the encoder with ImageNet weights [7] and adapting the network to scar segmentation using a limited labeled dataset of 15 images. These images were found online and manually segmented using the Image Labeler tool in MATLAB. The created dataset is augmented with rotations of 90, 180, and 270 degrees and different lighting conditions. The augmented dataset is then split into training and validation sets using a 90/10 ratio, and the model is trained for 50 epochs to achieve a convergence. Training was performed using a composite loss function combining multiclass Dice loss [8] and smoothed cross-entropy loss to balance region overlap accuracy with class stability. Optimization was carried out using the Adam optimizer, and model performance was monitored on the validation set each epoch, with the best performing model saved based on the minimum validation loss.

B. Post-Segmentation Processing

After segmentation is complete, the generated scar mask is smoothed with a gaussian blur and any small pieces of noise outside the main mask are removed. This "clean" scar mask is then covered with squares the size of the laser array, covering the entire scar and minimizing contact with normal skin. In the code, this is done by taking the top-left-most corner of

the scar mask and tiling the scar with squares, each new row starting at the left-most side of the scar. Once the tiling is complete, the squares are shifted so that the center of the line of squares is the center of the scar mask section they cover. To find a more optimal coverage, the image is rotated in one degree increments and then re-tiled with squares. The rotation with the least amount of squares used to cover the scar mask is then determined the most optimal in order to reduce time of surgery and unnecessary skin hits.

C. Heat Model

One important aspect of this surgery, regardless of whether the laser is ablative or not, is the surrounding tissue's temperature. The tissue is rapidly heated up and undergoes significant heat damage [5]. While targeted damage to encourage the body's healing factor to remodel the area is intentional, you must be careful not to overly damage the tissue. One way to ensure you don't harm the patient, is to regulate the overall temperature of the tissue. Thus, we developed a heat model to allow us to predict how the heat will dissipate through the hypertrophic scar into the free flowing air.

For the sake of this argument, we need to know the time it will take for the scar to be cooled to ambient temperature by free convection. Additionally, to simplify the scenario, we assume uniform thermal conductivity through the hypertrophic scar, skin, and fat layers. Furthermore, after confirming Biot's number proves the validity of the assumption, we utilize the lumped capacitance model to simplify the scenario even further. For the math confirming the validity of the lumped capacitance as well as to see the equation for temperature modeling, see appendix section F.

D. Path Planning

To identify an optimal path along the segmented scar's laser square layout that minimizes both heat damage and laser operation time, two path-planning approaches were evaluated: a greedy algorithm designed to reduce time and thermal exposure and a tabular Q-learning reinforcement learning method.

1) *Greedy Algorithm*: To provide a good baseline to compare to reinforcement learning, a greedy algorithm was written to minimize the time of surgery and prevent major (lasering an already-hit square) and minor (lasering a hot square) burns. For simplicity's sake, a scar square is ready to be hit without being burned after it is cooled down back to room temperature (after approximately 98.37 seconds).

The algorithm begins with a simulated laser agent acting as a robot, beginning at the origin and moving in Manhattan steps. At any decision point, the algorithm evaluates all the unlasered scar squares and computes a ready time for each which is equal to the maximum of the current time and the square's heat-affected time plus the cooldown period. A travel time from the current laser agent position to each square is estimated using Manhattan distance; it is assumed it takes the agent 0.2 seconds to travel 1 image pixel width. The next square to be lasered is selected by greedily minimizing the sum of the square's ready time and the agent's travel

time, corresponding to the earliest feasible arrival time without inducing burns. Once the target is selected, the agent advances to the chosen square and applies the laser array. The square itself is marked as lasered and all neighboring squares within a heat radius become heat affected. The heat radius of 1.5 times the laser size was arbitrarily chosen because the heat model only accounts for one dimensional conductive heat transfer out of the body. The heat-affected squares are ineligible for lasering until they cool down to room temperature. This process is repeated until all scar squares are treated, yielding a deterministic lasering order that works on all scar square layouts that balances travel efficiency with thermal safety constraints.

2) *Q-Learning and Reward Function:* Based on our lessons in class, we chose to explore reinforcement learning as a potential way to figure out the idea path that simultaneously minimizes potential burns, while taking the shortest path possible (by minimizing the distance between its actions). Specifically, we focused on Q-Learning as the method to determine the path. Q-Learning builds a table that correlates actions and potential states. It fills the table with values based on the outcome of the reward function for the given state/action pair. Over a series of episodes, our model will be able to learn the ideal next action given its current state.

Our reward function has a series of smaller rewards, in addition to a massive reward for the overall completion of the ultimate goal. We have a negative reward that is proportionally based on distance between the previous and current state; the closer the previous and current state are to each other, the smaller the negative reward. There are two rewards for burning the patient, a major burn has a largely negative reward, while a minor burn has a small negative reward. The major burn mainly serves to discourage accidentally hitting the same square twice, while the minor burn reward discourages hitting any square directly next to the current square. In addition to negatively discouraging the model away from burns, we positively reinforce the discovery of new squares with a reward for finding a square that hasn't been visited before. The final reward is a large reward for successfully hitting every single square.

The main drawback to this style of reinforcement learning, is the model must be re-trained on every single scar. Later in this paper, we will discuss our thoughts on potentially improving our model and getting around this issue.

III. PHYSICAL SYSTEM PREPARATION

A. End Effector Modeling

In the hopes of integrating our path planning algorithm with a real camera and UR5e, we created a custom end effector that could allow a camera to be mounted to the end of the UR5e as well as allow for the addition of Q-Tips to simulate a laser array. This end effector is far larger than the actual laser array, but would allow us to test with actual hardware with low stakes and on a nonexistent budget.

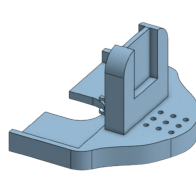


Fig. 1. End Effector CAD Model



Fig. 2. End Effector in Robotiq Gripper

IV. RESULTS

A. Segmentation Results

The best segmentation model was found to be the finetuned U-Net, with an average 96.43% accuracy on the validation dataset. The other models tested were so visually wrong or ineffective, the average accuracy of scar segmentation was not measured. Segmentation mask graphical results and discussion for these can be found in Appendices C, D, and E. A visual representation of the U-Net accuracy is shown in Figure 3.

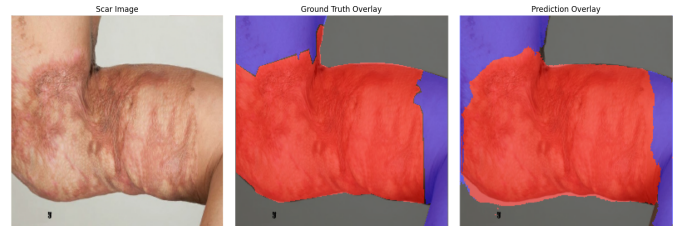


Fig. 3. U-Net Model Performance on Test Scar Image

Once the U-Net model was confirmed accurate, it was then post-processed through gaussian blur and square tiling. The result of this pipeline to prepare the mask for path planning is shown in Figure 4. This is assuming the laser is 24x24 pixels wide with respect to the image.



Fig. 4. Segmentation to Squares Pipeline

B. Path Planning Results

The quality of path planning was assessed based on total distance traveled by the laser agent (representing duration of the surgery) and number of major and minor burns given to the "patient" by the agent. These quantitative results are presented in Table I. A main positive is that neither path planning method severely burns the patient. However, it was shown that the greedy algorithm does perform better in the two non-equal metrics. This is likely because the greedy

algorithm is specifically designed to minimize these metrics and deterministically finds the optimal path that is incapable of burning the patient.

TABLE I
PATH PLANNING METHOD PERFORMANCE

Pathing Type	Performance Metric		
	Distance Traveled	Major Burns	Minor Burns
Greedy	3083px	0	0
RL	5092px	0	10

Another large benefit of the greedy algorithm is that it is applicable to every input scar image and does not need to be retrained with a new square layout. To its benefit, the Q-Learning approach does show promise for more complicated surgeries with less well defined constraints that cannot be easily minimized with a greedy algorithm.

Path planning results were statically visualized with the laser squares overlapping their respective image in numbered application order (Fig 5, Fig 6). These images are also dynamically visualized at the link in Appendix B.



Fig. 5. Lasering Order of the Greedy Algorithm

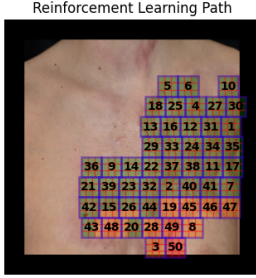


Fig. 6. Lasering Order of the Q-Learning Algorithm

V. LIMITATIONS AND FUTURE WORK

Our project, while informative, has several areas of improvement. For the segmentation model, the main limitation is a lack of training data. The best segmentation approach found was a U-Net fine-tuned on a very small amount of training data. However, the model would likely perform even better with a larger and more diverse image set for training. Another method that would likely be successful is creating our own model using the large training dataset, voiding the potential of a pretrained encoder adversely affecting predictions. While creating a unique model trained with only hypertrophic scar data would be ideal, we would need significantly more data to be able to produce our current levels of accuracy.

Meanwhile, on the reinforcement learning front, there are multiple limitations and areas of improvement. First off and foremost, our reward function needs additional fine-tuning. Our current model has more major burns and minor burns than is permissible for a successful surgery. Significant reward engineering would need to be undergone in order to perfect

our rewards. Since we are still seeing burns, we would likely need to further penalize our model for burning a patient, while increasing the positive reinforcement for successful path planning. Another major drawback of our model is that it must be retrained for every single scar. Our current method creates a Q-table that is unique for an individual scar, based on its unique square segmentation make-up. Thus, every single scar requires redoing segmentation, squaring, and then training the path planning model. There are three ways we could fix this issue. The first would be to implement Deep Q-Network (DQN) reinforcement learning for path planning and hope that we have enough data to create a more robust model. The second method would mean redoing our entire project thus far. Hypothetically, we could train a neural network to jump straight from an image of a scar to a planned path. We could actually use our current segmentation and squares to path planning pipeline to create training data for this hypothetical neural network that would replace our entire project. The final method of improving our path planning model would be to simply utilize the greedy algorithm that serves as our benchmark. The greedy algorithm should function for all potential scars without needing any additional training.

In terms of our physical system, our initial desire was to integrate our planned path into a simulated and physical UR5e system. However, as our segmentation, heat modeling, and path planning became greater challenges than expected, we moved away from our simulation and physical system. Ideally we would have continued refining our end effector, integrated the path planning into Gazebo simulation, and then begun testing actual UR5e movement. Instead, these actions should be taken to test our methodology in the future.

VI. CONCLUSION

This work demonstrates the feasibility of utilizing an autonomous robotic framework for laser-based hypertrophic scar treatment via the integration of scar segmentation, temperature modeling, and optimal path planning. By evaluating multiple segmentation approaches, this project shows that a fine-tuned U-Net can accurately identify scar regions despite limited scar data. Using mathematical heat modeling, the project was able to prove the concept is worth pursuing, and thus may be worth creating an experimental model to better demonstrate the heat dissipation. The proposed post-processing and tiling strategy, coupled with both greedy and reinforcement learning algorithms, successfully generates safe and effective treatment paths in a simulated surgical setting. While the greedy algorithm currently outperforms tabular Q-learning in efficiency and safety, the reinforcement learning approach highlights potential for more complex and less structured surgical scenarios, and could be more accurate with a Deep Q-Network approach. Although future work is required to address data limitations, improve learning-based generalization, and validate the system on physical hardware, this project establishes a strong foundation for future research in autonomous laser scar therapy and illustrates how robot learning can meaningfully contribute to safer, accessible care.

REFERENCES

- [1] B. Kuehlmann, Z. Stern-Buchbinder, D. C. Wan, J. S. Friedstat, and G. C. Gurtner, "Beneath the Surface: A Review of Laser Remodeling of Hypertrophic Scars and Burns," *Advances in Wound Care*, vol. 8, no. 4, pp. 168–176, 2019, doi: 10.1089/wound.2018.0857.
- [2] J. Kim, I. Oh, Y. N. Lee, et al., "Predicting the severity of postoperative scars using artificial intelligence based on images and clinical data," *Scientific Reports*, vol. 13, p. 13448, 2023, doi: 10.1038/s41598-023-40395-z.
- [3] "Blackdot — Welcome to the Tattoo Revolution," Blackdot, 2025. [Online]. Available: [\[https://blackdot.tattoo/\]\(https://blackdot.tattoo/\)](https://blackdot.tattoo/) [Accessed: 12-Dec-2025].
- [4] V. Penza, D. Salerno, A. Acemoglu, J. Ortiz, and L. S. Mattos, "Hybrid Visual Servoing for Autonomous Robotic Laser Tattoo Removal," in Proc. IEEE/RSJ Int. Conf. Intelligent Robots and Systems (IROS), Macau, China, 2019, pp. 4461–4466, doi: 10.1109/IROS40897.2019.8968000.
- [5] Klifto, Kevin M et al. "Laser management of hypertrophic burn scars: a comprehensive review." *Burns and trauma* vol. 8 tkz002. 16 Jan. 2020, doi:10.1093/burnst/tkz002
- [6] N. Ravi et al., "SAM 2: Segment Anything in Images and Videos," arXiv preprint arXiv:2408.00714, 2024.
- [7] K. He, X. Zhang, S. Ren, and J. Sun, "Deep residual learning for image recognition," arXiv:1512.03385 [cs.CV], 2015.
- [8] S. Kato and K. Hotta, "Adaptive t-vMF Dice Loss for Multi-class Medical Image Segmentation," arXiv preprint arXiv:2207.07842, 2022. [Online]. Available: <https://arxiv.org/abs/2207.07842>
- [9] T. L. Bergman, A. S. Lavine, F. P. Incropera, and D. P. DeWitt, *Fundamentals of Heat and Mass Transfer*, 7th ed. USA: John Wiley & Sons, 2011.
- [10] Hypertrophic Scar Royalty-Free Images, www.shutterstock.com/search/hypertrophic-scar. Accessed 20 Oct. 2025.
- [11] GeeksforGeeks, "What is Reinforcement Learning?," Nov. 7, 2025. [Online]. Available: <https://www.geeksforgeeks.org/machine-learning/what-is-reinforcement-learning/>

APPENDIX

A. GitHub Repository

To access the code for this project, please view the GitHub repository at <https://github.com/25Lilly/Path-Planning-for-Robotic-Hypertrophic-Laser-Scar-Therapy>.

B. Dynamic Visualizations

To view a Gif please go here: <https://github.com/25Lilly/Path-Planning-for-Robotic-Hypertrophic-Laser-Scar-Therapy/tree/main/Visualizations>

C. GMM Results and Discussion

The unsupervised GMM was tested on 10 scar images to see how it would perform on scar segmentation (Fig. 7). The results show that this unsupervised model works very well with sharp boundaries. However, given that hypertrophic scars vary widely in color and texture [2], this is not effective on all scar types, as is evident in the figure. It also lacks the ability to determine which segmented piece is the scar, something that would need another model tagged onto it to determine cluster type. This led to the method being viewed as ineffective due to the need for high clinical accuracy, which GMM does not provide. *

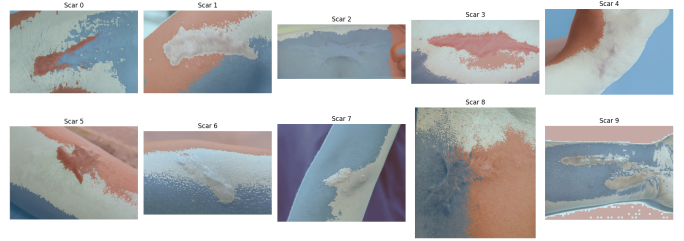


Fig. 7. GMM mask outputs

D. ResNet-18 Results and Discussion

The pretrained ResNet-18 spatial features model was tested on 10 scar images to see how it would perform on scar segmentation (Fig. 8). The results show that this pretrained model would likely never be accurate enough for clinical use, confirming our hypothesis. This is likely due to the fact that the pretrained model never saw any scars in its ImageNet training data [7]. This method would likely be improved with additional training data to fine-tune the model.

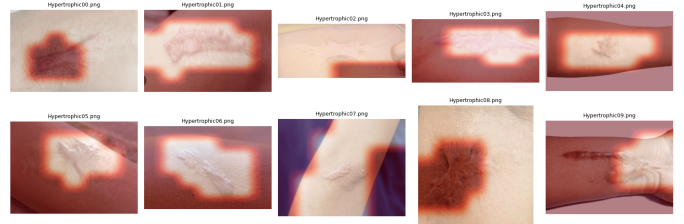


Fig. 8. Pretrained ResNet-18 mask outputs

E. SAM Results and Discussion

The SegmentAnything Model with checkpoint ViT-B only performed well on 20% of the test images (Fig 9). SAM with the ViT-H checkpoints performed better than the smaller model. However, it still performed very poorly, properly segmenting only 30% of the test scar images (Fig 10). Neither SAM output provided a solid mask able to be utilized in the square post-processing and path planning pipeline. This was deemed nowhere near clinically accurate enough for medical image segmentation. This could be improved with some fine tuning using hypertrophic scar data.



Fig. 9. SAM with ViT-B Checkpoint Segmentation Outputs

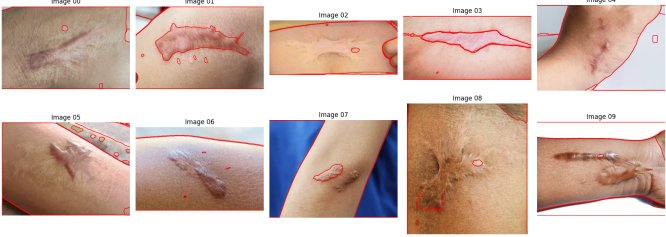


Fig. 10. SAM with ViT-H Checkpoint Segmentation Outputs

F. Heat Modeling Mathematical and Theoretical Background

1) Heat Constants:

$$h = 2 \frac{W}{m^2 * k} \quad (1)$$

$$L_c = 8 * 10^{-3} m \quad (2)$$

$$k \approx 0.3 \frac{W}{m * k} \quad (3)$$

$$\alpha = 22.5 * 10^{-6} \frac{m^2}{s} \quad (4)$$

This k value is assuming a standard skin/fat ratio, the value should be increased to account for thicker hypertrophic scars (aka due to increased collagen, likely in the range of 0.3-0.5)

2) Heat Math: Biot's Number Confirmation of Validity of Lumped Capacitance Model:

$$Bi = \frac{hL_c}{k} \quad (5)$$

Assuming our constants and situations, the lumped capacitance model is applicable for a Biot's number less than 0.1.

$$Bi = \frac{2 * 8^{-3}}{0.3} \quad (6)$$

$$Bi = 0.053 \quad (7)$$

Thus, based on this math, we can make the lumped capacitance approximation.

Lumped Capacitance Model:

$$\frac{T - T_\infty}{T_i - T_\infty} = e^{-\frac{hA_s}{\rho V c_p} t} \quad (8)$$

$$\frac{T - T_\infty}{T_i - T_\infty} = e^{-\frac{\alpha h}{k L_c} t} \quad (9)$$

$$T = T_\infty + (T_i - T_\infty)e^{-\frac{\alpha h}{k L_c} t} \quad (10)$$

When we plug all our hypothetical values for our given scenario into the given model, we find this equation.

$$T = 300K + (500K - 300K)e^{-\frac{22.5 * 10^{-6} \frac{m^2}{s} * 2 \frac{W}{m^2 * k} t}{0.3 \frac{W}{m * k} * 4 * 10^{-3} m}} \quad (11)$$

3) Visual Demonstration of Heat Model Dissipation Graph:

Figure 11 displays how the heat dissipates in a laser-affected region over time. The red line represents when we assume the region has cooled down and is back to a safe temperature.

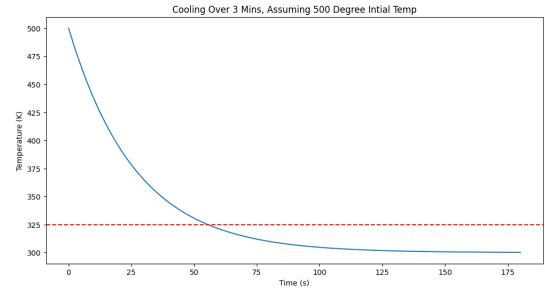


Fig. 11. Heat Dissipation Out of the Hypertrophic Scar after Laser Application

G. Reinforcement Learning Rewards

Figure 12 shows how the Q-learning table's rewards performed over training episodes. The large negative spikes are likely due to a major burn to the patient where the laser agent hit the subject in the same location twice.

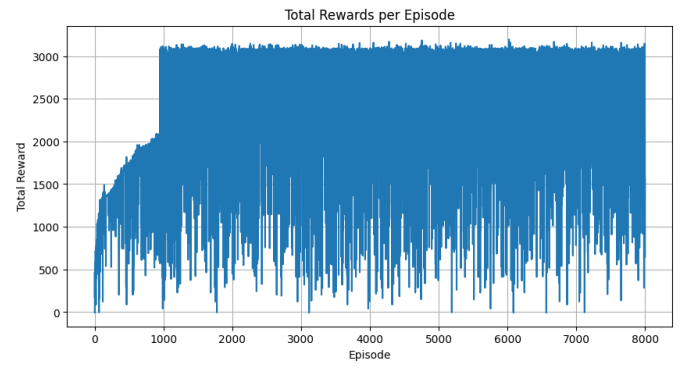


Fig. 12. Q-Table Reinforcement Learning Rewards over Episodes